Paper No. 125. (quote when citing this article)
Eleventh World Conference on Earthquake Engineering
ISBN: 0 08 042822 3

3D SIMULATIONS OF LONG-PERIOD STRONG GROUND MOTION IN SEDIMENTARY BASINS

Y. HISADA

Department of Architecture, Kogakuin University
Nishi-Shinjuku 1-24-2, Tokyo 163-91, Japan
TEL: 81-3-3342-1211 (Ext. 2726)
FAX: 81-3-3340-0140
E-mail: hisada@cc.kogakuin.ac.jp
http://kouzou.ns.kogakuin.ac.jp/hisada/home.html

ABSTRACT

In this study, we describe a Boundary Element Method (BEM) to simulate long-period strong ground motions in 3D basin structures consisting of multi-layers. Our BEM uses various newly developed techniques; asymptotic solutions of Green's function for layered spaces by Hisada (1995), and the Green's function library. This BEM produces numerically much more stable results without heavy computation than Hisada *et al.* (1993).

KEYWORDS

3D structure; Boundary Element Method; layered half-spaces; Green's function; Green function library, asymptotic solutions of Green's function; sedimentary basin; long-period strong ground motion

INTRODUCTION

Since the unprecedented damage in Mexico City and the Bay Area of San Francisco during recent earthquakes, it has been widely recognized that surface waves locally generated in sedimentary basins, have great influence on long-period structures, such as high-rise buildings, oil storage tanks, and long-span bridges. Recent observations using seismic array data have indicated that the generation and propagation of those surface waves are strongly affected by three dimensional structure of the basins (e.g., Frankel *et al.*, 1991; Kinoshita *et al.*, 1992). In order to simulate those surface waves in 3D structures, Finite Difference Methods (FDM) and Finite Element Methods (FEM), so far, have been most widely used (Toshinawa and Ohmachi, 1992; Frankel and Vidale, 1992; Graves, 1993; Yomogida and Etgen, 1993; Olsen *et al.*, 1995). However, the applications of those methods to large scale 3-D models require the huge amount of computer memory, CPU time, and pre- and post-processing. Also, we have to carefully check for the accumulation of numerical errors (e.g., numerical grid dispersion; see Frankel and Vidale, 1992).

On the other hand, the Boundary Element Methods (BEM) are an alternative choice for this purpose (e.g., Sanchez-Sesma and Luzon, 1995). It is well known that the BEMs have great advantages over FDM and FEM regarding the computer memory, the radiation condition, pre- and post-processing. However, it is not easy to extend the conventional BEMs, which are based on Green's functions for homogeneous spaces, to realistic multi-layered structures, because large number of boundary elements are required along the all boundaries between layers.

One way to solve this problem is to use the BEMs based on Green's functions and/or the normal mode solution for layered spaces (e.g., Hisada *et al.*, 1993). Hisada *et al.* (1993) developed a 3D BEM for layered spaces, and successfully simulated long-period strong ground motion (6 - 10 sec) for the Kanto and Los Angeles basins (Hisada *et al.*, 1993; Hisada, 1994). However, they used an simple assumption that

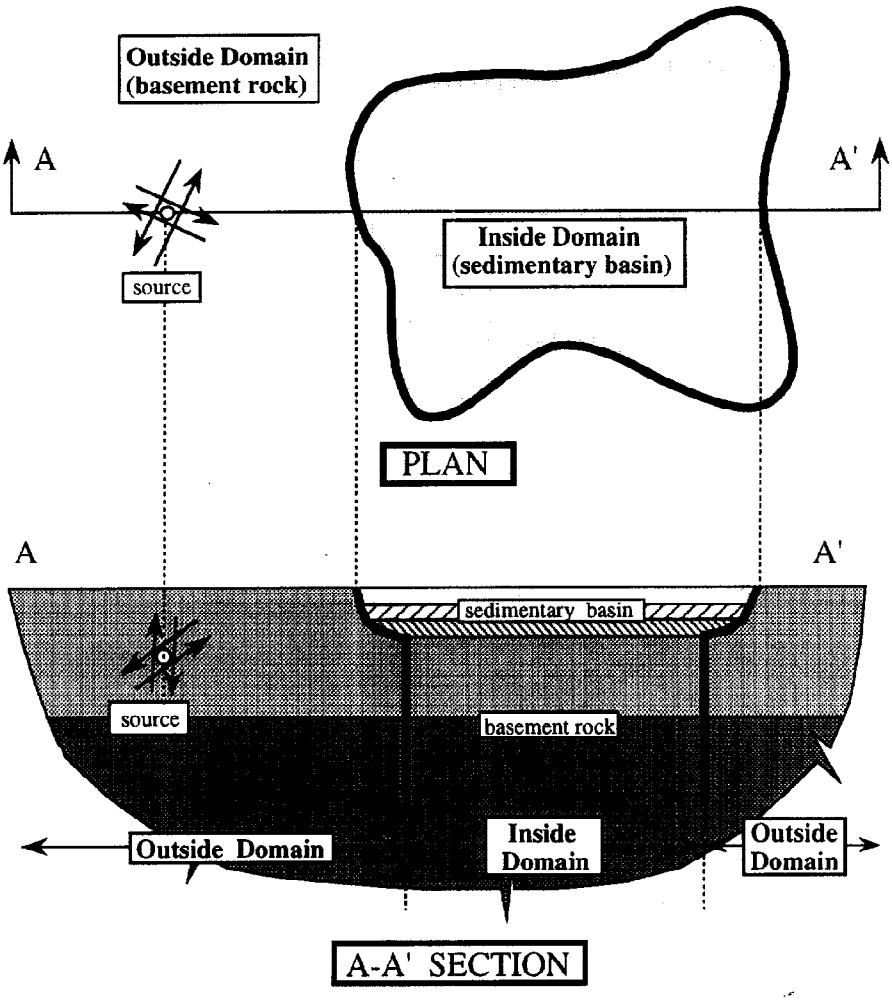

Fig.1. A 3D sedimentary basin model used in this study

the interfaces between the inside (basin) and outside (bedrock) structures as being vertical. In addition, they found their BEM has numerical instabilities, because 1) the integrands of the wavenumber integrations for computing Green's functions have extremely slow convergence, when a source and a receiver are located at similar depths; 2) they used the Haskell's propagator matrix for their Green's functions, which has inherently numerical instabilities at higher frequencies.

In this study, we will show a 3D BEM for layered structures using the newly developed Hisada's Green function (1995). First, this BEM is much more numerically stable than the previous, because the R/T matrix method is used. Second, the introduction of the asymptotic solutions by Hisada (1995) guarantees quick convergences of the integrands even for the cases that a source and a receiver are located at similar depths. Third, the asymptotic solutions eliminate the singularity problem of the BEM formulation. Finally, a Green function library technique is demonstrated, which greatly reduces the CPU time.

FORMULATION OF 3D BEM FOR LAYERED SPACES

Fundamental Equations for 3D BEM

We consider the system depicted in Fig.1 to model a 3D sedimentary basin structure. It consists of the inside and outside domains; the inside (basin) domain consisting of sedimentary layers overlying the crustal layers, and the outside (bedrock) domain of only crustal layers.

From the representation theorem, we get

$$C^b_{ik}(\mathbf{y})\, U_i^b(\mathbf{y}) + \int_{\Gamma_b} \left\{ P^{b*}_{ik}(\mathbf{x},\mathbf{y})\, U_i{}^b(\mathbf{x}) - U^{b*}_{ik}(\mathbf{x},\mathbf{y})\, P_i{}^b(\mathbf{x}) \right\} d\Gamma(\mathbf{x}) = U^{Ib}_k(\mathbf{y}), \tag{1}$$

$$C^b_{ik}(\mathbf{y}) = \delta_{ik} \int_{\Omega_b} \delta(\mathbf{x},\mathbf{y})\, d\Omega(\mathbf{x}) = -\int_{\Gamma_b} P^{b*}_{ik}(\mathbf{x},\mathbf{y})\, d\Gamma(\mathbf{x}), \tag{2}$$

for the bedrock (outside) domain, and

$$C^s_{ik}(\mathbf{y})\, U_i^s(\mathbf{y}) + \int_{\Gamma_b} \left\{ P^{s*}_{ik}(\mathbf{x},\mathbf{y})\, U_i{}^s(\mathbf{x}) - U^{s*}_{ik}(\mathbf{x},\mathbf{y})\, P_i{}^s(\mathbf{x}) \right\} d\Gamma(\mathbf{x}) = U^{Is}_k(\mathbf{y}), \tag{3}$$

$$C^s_{ik}(\mathbf{y}) = \delta_{ik} \int_{\Omega_s} \delta(\mathbf{x},\mathbf{y})\, d\Omega(\mathbf{x}) = -\int_{\Gamma} P^{s*}_{ik}(\mathbf{x},\mathbf{y})\, d\Gamma(\mathbf{x}), \tag{4}$$

for the sedimentary basin (inside) domain, where Γ_b is the boundary between the bedrock and the basin domains, **Y** is the source point on Γ_b and **X** is the observation point, U_i and P_i are the *i*th component of the displacement and the traction, and U^*_{ik} and P^*_{ik} are those of Green's functions for the layered half-space. The superscripts b and s represent the bedrock and sedimentary basin domains, respectively. $U^{Ib}_k(\mathbf{y})$ and $U^{Is}_k(\mathbf{y})$ are incident waves at **Y**, which can be the plane body waves, the surface waves, or the seismic waves from earthquake sources.

Green's function for layered half spaces

We adopt Hisada's Green function (1995), which has the following advantages:
1) It is numerically stable up to very high frequencies, because we adopted the R/T matrix method completely free from the exponential terms growing with frequencies (see e.g., Hisada, 1994).
2) The introduction of the asymptotic solutions can eliminate any difficulties for the wavenumber integration even for the cases that the depth of a source point is equal or close to that of an observation point (Hisada, 1995). Green's function in this case is expressed as the following simplified form

$$G(r,\theta,z;z_S) = \int_0^\infty \left[\{ d(z;z_S) - d^a(z;z_S) \} J(rk) dk + D^a(r,z;z_S) \right] S(\theta), \tag{5}$$

where G is displacement or traction Green's function assuming that the locations of a source and a receiver are at $(0,0,z_S)$ and (r,θ,z) in the cylindrical coordinate system, respectively, d is the original displacement-stress vector, d^a is its asymptotic solution which converges to d with increasing wavenumber, D^a is the analytical integration corresponding to d^a, J is a Bessel function, S is a sinusoidal function, and k is the horizontal wavenumber (see Hisada, 1994). The integrands can be easily numerically integrated, because the { } part quickly goes to zero with increasing k (see Hisada, 1995 for the details).

The FORTRAN programs for this Green's function are open to public use vie Internet. The address of the anonymous FTP site to obtain them is "coda.usc.edu" or "128.125.23.15", and the directory is "pub/hisada". Please check the README file in this directory first for the newest information.

Discretization

We discretize the boundary Γ_b into boundary elements. For the simplicity, we use the triangle elements with constant displacements and tractions. In this case, equation (1) can be

$$C^{bn}_{ik}\, U_i^{bn} + \sum_{m=1}^{M} \int_{\Gamma_{bm}} \{ P^{b*}_{ik}(\mathbf{x},\mathbf{y})\, U_i{}^{bm} - U^{b*}_{ik}(\mathbf{x},\mathbf{y})\, P_i{}^{bm} \} d\Gamma(x) = U_i^{Ibn}, \tag{6}$$

where m and n are the element numbers for the boundary element and the element with the source point **Y**, respectively, and M is the total number of the elements. Similarly, we get the equation for the basin domain corresponding to equation (3).

As shown in Fig.1, we can approximate Γ_b by truncating the BE discretization at a certain depth, that greatly reduces total number of boundary elements (see Hisada et al., 1993).

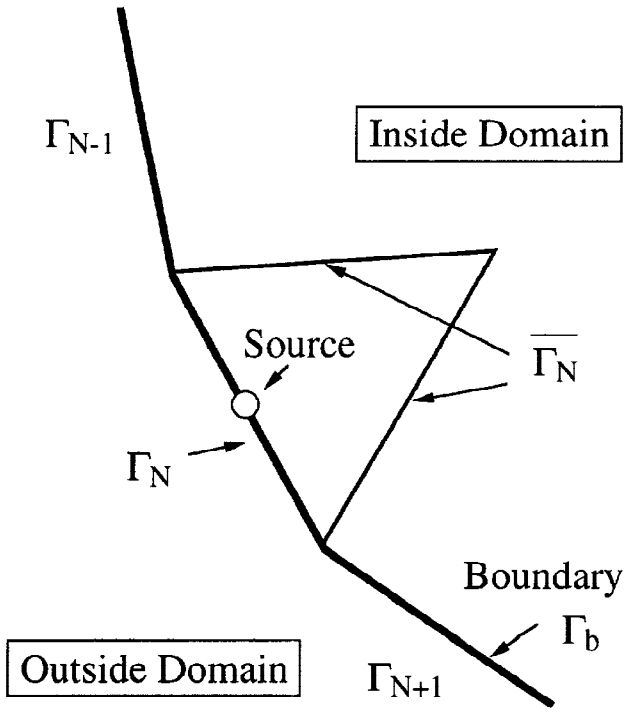

Fig.2. A local boundary Γ_L to evaluate coefficient C_{ik}^{bn} and to avoid the singularity problem

Coefficient C_{ik} and the Elimination of the Singularity problem

It is well known that the boundary integrations with P_{ik}^{*} in equation (6) have the singularity problem when m = n. This can be solved by considering both the integrations and the evaluations of coefficient C_{ik}, simultaneously (e.g., Rizzo *et al.*, 1985). When evaluating coefficient C_{ik}, we can simplify P_{ik}^{*} to a function including the singularly terms only, such as the static Green's functions. In this study, we adopt the Hisada's asymptotic solutions $D^a(r,\theta,z;z_S)$ in equation (5) as the simplified Green's functions, because, 1) they include the all singularity terms even for the case that a source point is located at layer boundaries, and 2) they are analytic solutions without the numerical wavenumber integrations (Hisada, 1995).

In this case, equation (6) can be

$$C_{ik}^{bn} = -\int_{\Gamma_b} P_{ik}^{b*}(\mathbf{x},\mathbf{y})\, d\Gamma(\mathbf{x}) = -\int_{\Gamma_L} P_{ik}^{ba}(\mathbf{x},\mathbf{y})\, d\Gamma(\mathbf{x}), \tag{7}$$

where P_{ik}^{ba} is Hisada's asymptotic solution corresponding to the traction Green's function. It is easily confirmed that Γ_L is not necessary to be Γ_b, and can be a local boundary covering an arbitrary small domain including the source point **Y**. This is a very useful fact for our formulation, because we will approximate Γ_b by truncating the BE discretization at a certain depth, and the approximate Γ_b would not evaluate the exact value of C_{ik}^{bn}.

As shown in Fig.2, we divide Γ_L into the two parts; one is the part of Γ_L on Γ_b (= Γ_n; the boundary element with the source point) and the other is the rest of Γ_L (= $\overline{\Gamma_n}$). Then, equation (7) will be

$$C_{ik}^{bn} = -\int_{\Gamma_L} P_{ik}^{ba}(\mathbf{x},\mathbf{y})\, d\Gamma(\mathbf{x}) = \overline{C_{ik}^{bn}} - \int_{\Gamma_n} P_{ik}^{ba}(\mathbf{x},\mathbf{y})\, d\Gamma(\mathbf{x}), \tag{8}$$

where,

$$\overline{C_{ik}^{bn}}(\mathbf{y}) = -\int_{\overline{\Gamma_n}} P_{ik}^{ba}(\mathbf{x},\mathbf{y})\, d\Gamma(\mathbf{x}) \ . \tag{9}$$

Note that the all singularity terms are in the integration of equation (8), but not equation (9). Finally, substituting equation (8) into equation (6), we get

$$\overline{C_{ik}^{bn}}\, U_i^{bn} + \sum_{m=1}^{M} \int_{\Gamma_{bm}} \{P_{ik}^{b*}(\mathbf{x},\mathbf{y})U_i^{bm} - \delta_{mn}P_{ik}^{ba*}(\mathbf{x},\mathbf{y})U_i^{bn} - U_{ik}^{ba}(\mathbf{x},\mathbf{y})P_i^{bn}\}d\Gamma(\mathbf{x}) = U_k^{Ibn} \ , \tag{10}$$

where,

$$\delta_{mn} = \left\{ \begin{array}{l} 1 \text{ (for } m=n) \\ 0 \text{ (for } m\neq n) \end{array} \right\}. \tag{11}$$

In equation (10), there are no singularity problems, because, when m = n (X = Y), the all singularities in P_{ik}^{b*} are subtracted by P_{ik}^{ba}. The same formulation is applied for the inside domain.

Note that a boundary element must be within a layer and cannot cross layer boundaries in the formulation presented in this paper. This is because, in the source layer, the Hisada's asymptotic solutions consist of the direct waves from the source point and the reflected waves from the source layer's boundaries, which represents physically appropriate wavefield in this layer. However, in a layer next to the source layer, the solutions consist of only the transmitted waves from the source layer and lack the reflected waves (see Hisada, 1995). Therefore, if an element crosses a layer boundary, the Hisada's solution does not represent appropriate wavefield in the part crossing the boundary.

Matrix Representation and Linear Equations

Equation (10) can be expressed by matrix forms,

$$\sum_{m=1}^{M} \left(\left[\Delta P^{bnm}\right]\left\{U^{bm}\right\} - \left[\Delta U^{bnm}\right]\left\{P^{bm}\right\} \right) = \left\{U^{Ibn}\right\}, \tag{12}$$

where,

$$\left\{U^{bm}\right\} = \left\{ \begin{array}{c} U_x^{bm} \\ U_y^{bm} \\ U_z^{bm} \end{array} \right\}, \quad \left\{P^{bm}\right\} = \left\{ \begin{array}{c} P_x^{bm} \\ P_y^{bm} \\ P_z^{bm} \end{array} \right\}, \quad \left\{U^{Ibn}\right\} = \left\{ \begin{array}{c} U_x^{Ibn} \\ U_y^{Ibn} \\ U_z^{Ibn} \end{array} \right\},$$

$$\left[\Delta U^{bnm}\right] = \left[\begin{array}{ccc} \Delta U_{xx}^{bnm} & \Delta U_{yx}^{bnm} & \Delta U_{zx}^{bnm} \\ \Delta U_{xy}^{bnm} & \Delta U_{yy}^{bnm} & \Delta U_{zy}^{bnm} \\ \Delta U_{xz}^{bnm} & \Delta U_{yz}^{bnm} & \Delta U_{zz}^{bnm} \end{array} \right], \left[\Delta P^{bnm}\right] = \left[\begin{array}{ccc} \Delta P_{xx}^{bnm} & \Delta P_{yx}^{bnm} & \Delta P_{zx}^{bnm} \\ \Delta P_{xy}^{bnm} & \Delta P_{yy}^{bnm} & \Delta P_{zy}^{bnm} \\ \Delta P_{xz}^{bnm} & \Delta P_{yz}^{bnm} & \Delta P_{zz}^{bnm} \end{array} \right],$$

$$\Delta P_{ik}^{bnm} = \delta_{nm}\, \overline{C_{ik}^{bn}} + \int_{\Gamma_{bm}} \left\{ P_{ik}^{b*}(\mathbf{x},\mathbf{y}) - \delta_{nm}\, P_{ik}^{ba}(\mathbf{x},\mathbf{y}) \right\} d\Gamma(\mathbf{x}) \text{ , and}$$

$$\Delta U_{ik}^{bnm} = \int_{\Gamma_{bm}} U_{ik}^{b*}(\mathbf{x},\mathbf{y}) d\Gamma(\mathbf{x}) \ . \tag{13}$$

Changing n from 1 to M in equation (12), we get a matrix equation

$$\left[\Delta P^{b}\right]\left\{U^{b}\right\} - \left[\Delta U^{b}\right]\left\{P^{b}\right\} = \left\{U^{Ib}\right\}, \tag{14}$$

for the bedrock domain, where,

$$\begin{aligned} \left\{U^{b}\right\} &= \left\{ \left(U_x^{b1}, U_y^{b1}, U_z^{b1}\right), \left(U_x^{b2}, U_y^{b2}, U_z^{b2}\right), \ldots, \left(U_x^{bM}, U_y^{bM}, U_z^{bM}\right) \right\}^T, \\ \left\{P^{b}\right\} &= \left\{ \left(P_x^{b1}, P_y^{b1}, P_z^{b1}\right), \left(P_x^{b2}, P_y^{b2}, P_z^{b2}\right), \ldots, \left(P_x^{bM}, P_y^{bM}, P_z^{bM}\right) \right\}^T, \\ \left\{U^{Ib}\right\} &= \left\{ \left(U_x^{Ib1}, U_y^{Ib1}, U_z^{Ib1}\right), \left(U_x^{Ib2}, U_y^{Ib2}, U_z^{Ib2}\right), \ldots, \left(U_x^{IbM}, U_y^{IbM}, U_z^{IbM}\right) \right\}^T, \end{aligned} \tag{15}$$

and

$$\left[\Delta U^b\right] = \begin{bmatrix} \left[\Delta U^{b11}\right] & \cdots & \left[\Delta U^{b1M}\right] \\ \vdots & \ddots & \vdots \\ \left[\Delta U^{bM1}\right] & \cdots & \left[\Delta U^{bMM}\right] \end{bmatrix},$$

$$\left[\Delta P^b\right] = \begin{bmatrix} \left[\Delta P^{b11}\right] & \cdots & \left[\Delta P^{b1M}\right] \\ \vdots & \ddots & \vdots \\ \left[\Delta P^{bM1}\right] & \cdots & \left[\Delta P^{bMM}\right] \end{bmatrix}. \tag{16}$$

Similarly, we get

$$\left[\Delta P^s\right]\{U^s\} - \left[\Delta U^s\right]\{P^s\} = \{U^{Is}\}, \tag{17}$$

for the sedimentary basin domain.

The linear equation for the tractions along the interface (Γ_b) between the two domains is obtained from equation (14) and (17) and is expressed as

$$\left(\left[\Delta P^s\right]\left[\Delta P^b\right]^{-1}\left[\Delta U^b\right] + \left[\Delta U^s\right]\right)\{P^s\} = \left[\Delta P^s\right]\left[\Delta P^b\right]^{-1}\{U^{Ib}\} - \{U^{Is}\}. \tag{18}$$

The displacement is obtained by

$$\{U^s\} = -\left[\Delta P^b\right]^{-1}\left[\Delta U^b\right]\{P^s\} + \left[\Delta P^b\right]^{-1}\{U^{Ib}\}, \tag{19}$$

where we used

$$\{U^b\} = \{U^s\}, \text{ and } \{P^b\} = -\{P^s\}. \tag{20}$$

Finally, displacements at arbitrary points are computed by substituting the displacement (19) and traction (18) on Γ_b into the representation theorem. For example, displacement at **Y** in the bedrock domain is expressed by

$$U_i^b(\mathbf{y}) = U_k^{Ib}(\mathbf{y}) - \int_{\Gamma_b} \left\{P_{ik}^{b*}(\mathbf{x},\mathbf{y})\, U_i^b(\mathbf{x}) - U_{ik}^{b*}(\mathbf{x},\mathbf{y})\, P_i^b(\mathbf{x})\right\} d\Gamma(\mathbf{x}). \tag{21}$$

Also we get $U_i^s(\mathbf{y})$ using the same procedure.

Green Function Library

In our BEM, most CPU time is consumed for computing Green's functions for layered half-space, because a huge number of the wavenumber integration (15) is needed for the all combinations of sources and receivers along the boundary, possibly millions for large scale basin models.

One of the best ways to reduce the CPU time is to construct the Green function library first, and then to start BEM computations using the library values and interpolation techniques. This technique has been using for the inversion analysis of earthquake source modelings (e.g., Wald and Heaton., 1994). From equation (15), Green's function for layered half-spaces can be

$$G(r,\theta,z;z_S) = \int_0^\infty \left[\{d(z;z_S) - d^a(z;z_S)\}J(rk)dk + D^a(r,z;z_S)\right] S(\theta) = L(r,z;z_S)\, S(\theta)\ , \tag{22}$$

Note that the sinusoidal function in equation (22) is out of the wavenumber integration. Therefore, what we construct is a 2D library $L(r,z;z_S)$ regarding z and r, but not a 3D library.

As an example, Fig.3 shows the real and imaginary parts of three components in a library $L(r,z;z_S)$ using a three layered model. As expected, receivers closer to the source point have larger amplitude.

CONCLUDING REMARKS

We showed a new 3D BEM for layered spaces, in which we used various new techniques: Green's function and its asymptotic solution by Hisada (1995), and the Green library. We will show some results for applying this BEM to actual sedimentary basins at the conference.

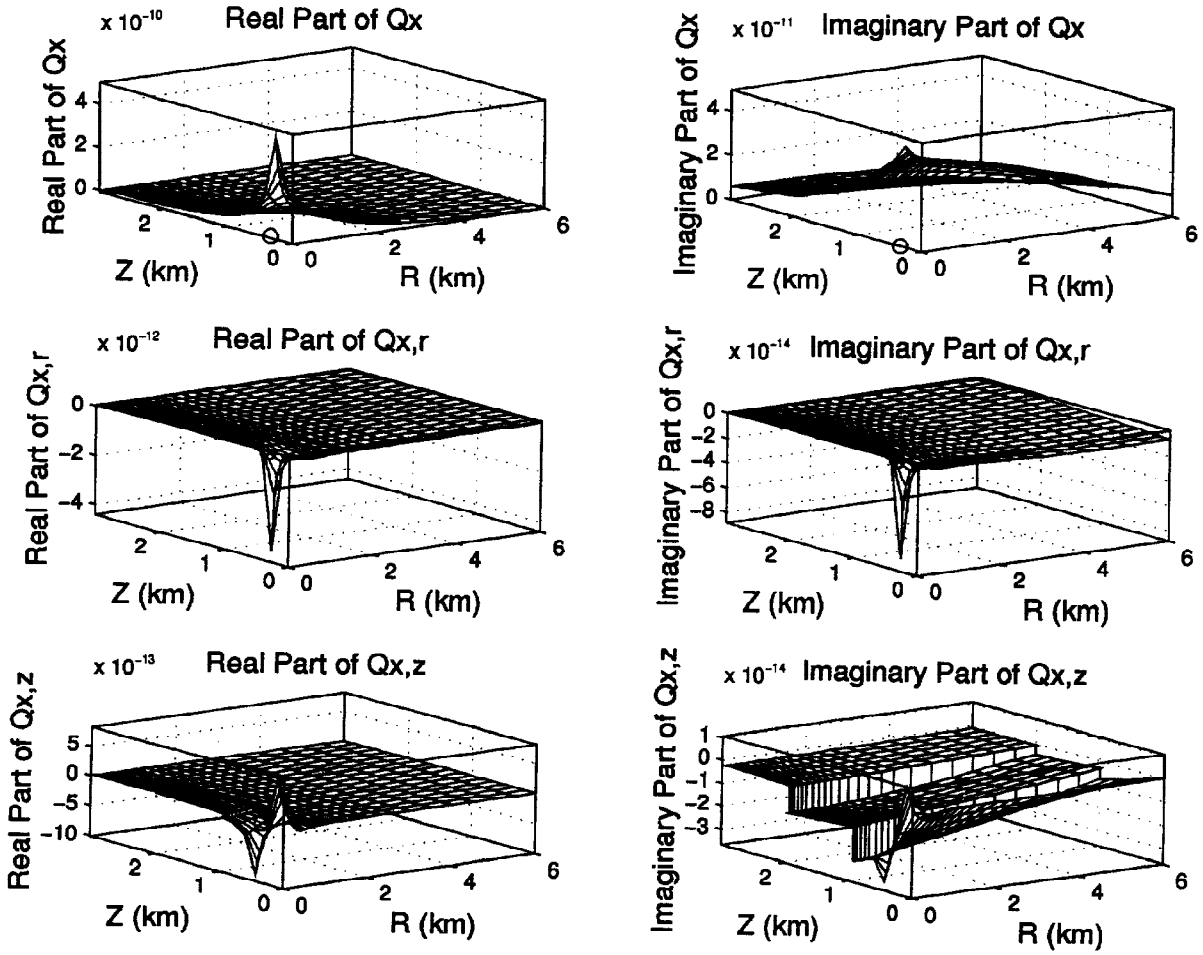

Fig.3. An example for a Green's function libray using a three-layered structure. The real and imaginary parts of Q_x, $Q_{x,r}$, and $Q_{x,z}$ are shown as the functions of z and r (see Hisada, 1995, for the details). The circles in the figures are the location of the source point.

REFERENCES

Frankel, A., S. Hough, P. Friberg, and R. Busby (1991). Observations of Loma Prieta aftershocks from a dense array in Sunnyvale, California, Bull. Seism. Soc. Am., **81**, 1900-1922.

Frankel, A., and J. Vidale (1992). A three-dimensional simulation of seismic waves in the Santa Clare valley, California, from a Loma Prieta aftershock, Bull. Seism. Soc. Am., **82**, 2045-2074.

Graves, R. W., (1993). Modeling three-dimensional site response effects in the Marina district basin, San Francisco, California, Bull. Seism. Soc. Am., **83**, 1042-1063.

Hisada, Y. (1994). An efficient method for computing Green's functions for a layered half-space with sources and receivers at close depths, Bull. Seism. Soc. Am., **84**, 1456-1472.

Hisada, Y. (1994). 3D simulations of long-period strong ground motion in the Los Angeles basin, Proc. of the 9th Japan Earthquake Engineering Symposium, Vol. 3, 115-120

Hisada, Y. (1995). An efficient method for computing Green's functions for a layered half-space with sources and receivers at close depths (Part 2), Bull. Seism. Soc. Am., **85**, 1080-1093.

Hisada, Y., K. Aki, and T.-L. Teng (1993). 3-D simulations of the surface wave propagation in the Kanto sedimentary basin, Japan (Part 2: Application of the surface wave BEM), Bull. Seism. Soc. Am., **83**, 1700-1720.

Kinoshita, S., H. Fujiwara, T. Mikoshiba, and T. Hoshino (1992). Secondary Love waves observed by a strong-motion array in the Tokyo lowland, Japan, J. Phys. Earth, **40**, 99-116.

Olsen, K.B., R.J. Archuleta, and J.R. Matarese (1995). Magnitude 7.75 Earthquake on the San Andreas Fault: Three-Dimensional Ground Motion in Los Angeles, Science, Dec.

Rizzo, F.J., D.J. Shippy, and M. Rezayat (1985). A boundary integral equation method for radiation and scattering elastic waves in three dimensions, International J. for Numerical Methods in Engineering, **21**, 115-129

Sanchez-Sesma, F.J., and F. Luzon (1995). Seismic response of 3D alluvial valleys for incident P, S and Rayleigh waves, Bull. Seism. Soc. Am., **85**, 269-284

Toshinawa, T., and T. Ohmachi (1992). Love wave propagation in a three-dimensional sedimentary basin, Bull. Seism. Soc. Am., **82**, 1661-1677.

Wald., D.J., and T.H. Heaton (1994). Spatial and temporal distribution of slip for the 1992 Landers, California, earthquake, Bull. Seism. Soc. Am., **84**, 668-691

Yamamoto, S., Y. Hisada, and S. Tani (1992). Simulations of long-period strong ground motions during the 1990 Upland earthquake, California, Proc. 9th World Conf. of Earhq. Engng.

Yomogida, K., and J. T. Etgen (1993). 3-D wave propagation in the Los Angeles basin for the Whittier-Narrows earthquake, Bull. Seism. Soc. Am., **83**, 1325-1345.